



Bayesian Population Model of the Pharmacokinetics of Venetoclax in Combination with Rituximab in Patients with Relapsed/Refractory Chronic Lymphocytic Leukemia: Results from the Phase III MURANO Study

Rong Deng^{1,7} · Leonid Gibiansky² · Tong Lu¹ · Priya Agarwal¹ · Hao Ding¹ · Xiaobin Li¹ · Smita Kshirsagar¹ · Dan Lu¹ · Chunze Li¹ · Sandhya Girish¹ · Jue Wang¹ · Michelle Boyer³ · Kathryn Humphrey³ · Kevin J. Freise⁴ · Ahmed Hamed Salem⁴ · John F. Seymour⁵ · Arnon P. Kater⁶ · Dale Miles¹

Published online: 18 June 2019
© Springer Nature Switzerland AG 2019

Abstract

Background Venetoclax is a selective B-cell lymphoma-2 (BCL-2) inhibitor approved for use as monotherapy or with rituximab in patients with chronic lymphocytic leukemia (CLL). The objectives of the current analysis of observed data from adult patients randomized to venetoclax–rituximab in the phase III MURANO study were to characterize venetoclax pharmacokinetics (PKs) using a Bayesian approach, evaluate whether a previously developed population PK model for venetoclax can describe the PKs of venetoclax when administered with rituximab, and to determine post hoc estimates of PK parameters for the exposure–response analysis.

Methods Parameter estimates and uncertainty estimated by a population PK model were used as priors. Additional covariate effects (CLL risk status, geographic region, and 17p deletion [del(17p)] status) were added to the model. The updated model was used to describe venetoclax PKs after repeated dosing in combination with rituximab, and to determine post hoc estimates of PK parameters for exposure–response analysis.

Results The PK analysis included 600 quantifiable venetoclax PK samples from 182 patients in the MURANO study. Model evaluation using standard diagnostic plots, visual predictive checks, and normalized prediction distribution error plots indicated no model deficiencies. There was no significant relationship between venetoclax apparent clearance (CL/F) and bodyweight, age, sex, mild and moderate hepatic and renal impairment, or coadministration of weak cytochrome P450 3A inhibitors. The chromosomal abnormality del(17p) and CLL risk status had no apparent effect on the PKs of venetoclax. A minimal increase in venetoclax CL/F (approximately 7%) was observed after coadministration with rituximab. CL/F was 30% lower in patients from Central and Eastern Europe ($n = 60$) or Asia ($n = 4$) compared with other regions (95% confidence interval [CI] 21–39%). Apparent central volume of distribution was 30% lower (95% CI 22–38%) in females ($n = 56$) compared with males ($n = 126$). No clinically significant impact of region or sex was observed on key safety and efficacy outcomes.

Conclusions The Bayesian model successfully characterized venetoclax PKs over time and confirmed key covariates affecting PKs in the MURANO study. The model was deemed appropriate for further use in simulations and for generating individual patient PK parameters for subsequent exposure–response evaluation.

Electronic supplementary material The online version of this article (<https://doi.org/10.1007/s40262-019-00788-8>) contains supplementary material, which is available to authorized users.

✉ Rong Deng
deng.rong@gene.com

Extended author information available on the last page of the article

1 Introduction

Venetoclax is a selective inhibitor of the B-cell lymphoma-2 (BCL-2) protein [1] that was originally approved for monotherapy as 400 mg daily oral dosing in patients with chronic lymphocytic leukemia (CLL) with the chromosomal abnormality 17p deletion [del(17p)] and a history of prior treatment [2]. Approval has since been expanded to include monotherapy or combination therapy with rituximab for patients

Key Points

The Bayesian population pharmacokinetic (PK) modeling approach provided a fast, efficient method to characterize venetoclax concentration–time profiles in combination with rituximab.

The findings from the model were consistent with a legacy population PK model and the analysis of observed venetoclax concentrations from the MURANO study.

The model was deemed appropriate for generating post hoc exposure parameters for further use in simulations, or for evaluation of exposure–response relationships.

with CLL or small lymphocytic lymphoma (SLL) with or without del(17p) after at least one prior therapy [3].

The pharmacokinetic (PK) characteristics of venetoclax are well established [4–7]. After oral administration, peak plasma concentrations (C_{\max}) are achieved within 5–8 h [8]. The drug is highly bound to plasma proteins; metabolism is chiefly via cytochrome P450 (CYP) 3A4 [4, 9–12]. Excretion is > 99.9% through the fecal route, indicating predominantly hepatic clearance (CL) [13].

A venetoclax legacy population PK model was previously developed using plasma samples from 505 subjects (including 50 with rituximab coadministration) enrolled in eight clinical studies, investigating the effect of patient characteristics and other factors on venetoclax PKs [6, 14]. The data showed that plasma venetoclax is described by a two-compartment PK model with first-order absorption and elimination. The venetoclax terminal elimination half-life ($t_{1/2}$) was approximately 26 h, and apparent CL (CL/F) was reduced by 19% and 84%, respectively, by moderate and strong inhibitors of CYP3A; weak inhibitors and inducers had no effect on CL/F . Rituximab coadministration increased venetoclax CL/F by an estimated 21%. Organic anion transporting polypeptide (OATP) 1B3 hepatic uptake transporter inhibitors decreased venetoclax CL/F by 15%. Women had a 32% lower apparent central volume of distribution (V_2/F) than men, and food increased bioavailability 2.99- to 4.25-fold over fasting for different food compositions (low-fat to high-fat). Venetoclax PKs were not affected by mild to moderate hepatic or renal impairment, body-weight, age, race, OATP1B1 transporter phenotype, P-glycoprotein (P-gp), breast cancer resistance protein (BCRP), or OATP1B1 modulators [6].

The ongoing randomized, open-label, phase III MURANO study (NCT02005471) includes 389 patients with relapsed/refractory CLL randomized to receive (1) venetoclax 400 mg daily for up to 2 years from cycle 1 day 1 (C1D1) with the addition of rituximab for the first

6 months, or (2) bendamustine plus rituximab for 6 months only [15]. The hazard ratio for progression or death was 0.17 (95% confidence interval [CI] 0.11–0.25; $p < 0.001$) at the primary analysis. Benefit was maintained across all clinical and biologic subgroups, including patients with del(17p) [15].

Using data from venetoclax–rituximab-treated patients in MURANO, the objectives of the present research were to characterize the PKs of venetoclax using Bayesian analysis, to compare with previously generated PK parameters [6, 14] and to identify any new covariates. The updated model was also used to determine post hoc estimates of PK parameters for exposure–response analysis.

2 Methods

2.1 Patients and PK Sampling

MURANO was conducted in accordance with the Declaration of Helsinki and the International Conference on Harmonisation of Good Clinical Practice guidelines [16, 17], and the trial protocol was approved by Institutional Review Boards. Eligible patients were aged ≥ 18 years, with relapsed/refractory CLL, and had received one to three previous treatments [15]. To reduce the incidence of tumor lysis syndrome (TLS) in the venetoclax–rituximab arm, a 5-week venetoclax dose ramp-up was administered to reach a target dose of 400 mg daily. After ramp-up, concomitant single infusions of intravenous rituximab were administered on D1 of each 28-day cycle for up to six cycles (375 mg/m² C1; 500 mg/m² subsequent cycles). Daily oral venetoclax 400 mg was scheduled for a fixed period of up to 2 years [15].

Plasma samples were taken from the venetoclax–rituximab arm for PK analysis before and 4 h after venetoclax dosing on C1D1 (after completion of the dose ramp-up) and C4D1. Additional samples were taken in the event of early withdrawal from the study or onset of TLS.

2.2 Analytical Methods

Plasma venetoclax concentrations were determined using validated liquid chromatography methods with tandem mass spectrometry [6]. The lower limit of quantification (LLOQ) for venetoclax was 2.08 or 2.18 ng/mL (depending on the individual sample analysis run).

2.3 Observed Venetoclax Pharmacokinetics (PKs)

Summary statistics for individual observed PK concentrations included mean, geometric mean, standard deviation (SD), coefficient of variation, median, minimum, and

maximum. The potential impact of rituximab on venetoclax PKs was assessed by evaluating the geometric mean ratio (GMR) of individual patient plasma venetoclax predose concentrations on C4D1 (after starting rituximab), compared with C1D1 (before starting rituximab).

2.4 Population PK Modeling

Legacy model parameter estimates, including all fixed, random, and covariate effects, were used as Bayesian priors to fit MURANO venetoclax PK data. The variance–covariance matrix of the parameter estimates of the legacy model was used to define the uncertainty for the priors. Priors were set using the NONMEM PRIOR subroutine with the TNPRI option and MSF file from the legacy model. The PRIOR subroutine allows NONMEM to introduce a penalty function for the estimation of the objective function value, based on the prior distribution of the parameters previously established. This penalty function uses a multivariate normal distribution for theta, omega, and sigma [18].

The legacy model covariates were moderate and strong CYP3A inhibitors (time-variant on CL/F); rituximab coadministration (time-variant on CL/F); coadministration of medications reported to be OATP1B3 transporter inhibitors (time-variant on CL/F); sex and subject population (i.e. patients vs. healthy volunteers on V_2/F); dose (using the power model with a reference value of 400 mg, time-variant on relative bioavailability [$F1$]); and food (fasted or fed, and low-, moderate-, or high-fat meal on $F1$ [the low-fat meal effect on $F1$ is 1]). This model is the same as the published venetoclax population model [6], except for fixing the OATP1B3 transporter inhibitor effects on CL/F as described previously [14].

In the present Bayesian analysis, model parameters were estimated with new data from the venetoclax–rituximab arm of MURANO using Bayesian prior distributions. The following additional new covariates, which were stratification factors for randomization in MURANO, were tested: del(17p) mutation status; geographic region (US/Canada [region 1], Australia/New Zealand [region 2], Western Europe [region 3], Central and Eastern Europe [region 4], Asia [region 5]); and disease responsiveness to prior therapy (i.e. CLL risk status). No priors were set for the new covariates. Missing continuous covariates were imputed as the median value of the covariate, while missing categorical covariates were imputed using the most frequent population value. No covariates had a missing data fraction exceeding 15%.

2.5 Model Development and Evaluation

The legacy model [6], with the addition of OATP1B3 transporter inhibitor effects on CL/F , was fitted to the new dataset

with informative prior distributions assigned. All parameters, including covariate effects, were re-estimated. Covariates investigated in the legacy analysis and not included in the legacy model were not re-tested. For technical reasons specific to NONMEM implementation, OATP1B3 transporter inhibitor effects on CL/F were fixed to the estimate of the legacy model [14]; this is equivalent to setting very informative priors on this parameter. The new covariates of interest [del(17p) status, geographic region, and CLL risk status] were then tested on CL/F and $F1$, two key PK parameters to determine exposure (i.e. area under the curve of plasma concentration versus time at steady state [AUC_{ss}]) for orally administered venetoclax. All other model parameters were re-estimated using the same Bayesian population PK approach, with non-informative flat priors set for the new covariates. As in the legacy analysis, new covariate–parameter relationships were investigated using a forward addition/backward elimination procedure, where a significance level of $\alpha = 0.01$ was used for forward addition and $\alpha = 0.001$ was used for backward elimination based on the likelihood ratio test.

Unlike models without priors (where one level of a categorical covariate serves as a reference), the effect of each level of a categorical covariate was tested individually and simultaneously within the same run. If the objective function change was below the critical value of 6.64, the covariate effect was rejected. Even though more than one covariate level was tested in each model, the critical value of the objective function change of 6.64 for one parameter at a significance level of $\alpha = 0.01$ was used, ensuring that no one parameter changed the objective function by more than this critical value. If the objective function change exceeded the critical value of 6.64, the effects of each covariate level were further investigated by removing the effects one by one or by grouping several levels together.

All parameter estimates were reported with a measure of uncertainty (standard error [SE] and relative standard error [RSE] obtained from the NONMEM covariance step). The final model was assessed using graphical evaluation, prediction-corrected visual predictive checks (VPCs) [19, 20], and normalized prediction distribution error (NPDE) plots [21] (see electronic supplementary material). Additional model comparison plots were also evaluated to compare predictions from competing models (see electronic supplementary material). VPCs were based on 500 simulated datasets. PK parameters and steady-state exposures were computed from the final model and summarized overall or after stratification by covariates.

The analysis was conducted using nonlinear mixed-effects modeling with NONMEM software version 7.3.0 (ICON Development Solutions, Ellicott City, MD, USA) [22]. The first-order conditional estimation method with interaction

(FOCEI) that utilized the PRIOR subroutine with the TNPRI option was applied for all NONMEM model runs.

2.6 Prediction of Individual PK Parameters

Individual PK parameters included CL/F , $F1$, V_2/F , and CL/F to $F1$ ratio (the determinant of AUC_{ss}). Individual steady-state exposures at 400 mg daily were also predicted. C_{max} at steady state ($C_{max,ss}$), trough plasma concentration at steady state ($C_{trough,ss}$), and AUC_{ss} were computed from the final model using empirical Bayes (post hoc) estimates.

3 Results

3.1 Observed Venetoclax PKs in MURANO

The GMR of predose venetoclax concentrations on C4D1 (after three 28-day cycles of rituximab) versus C1D1 (after ramp-up and before rituximab initiation) was 1.06, which was not statistically different from 1 ($p > 0.05$) (Fig. 1). The

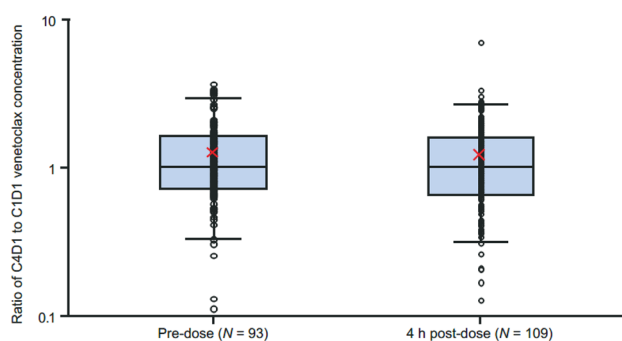


Fig. 1 Box plots of ratios of C4D1 to C1D1 venetoclax plasma concentrations by nominal timepoint: pharmacokinetic-evaluable population receiving actual dose of venetoclax 400 mg. Horizontal line represents the median; box represents Q1 (25th percentile) and Q3 (75th percentile); whiskers represent the 5th and 95th percentiles; and X represents the mean. C4D1 cycle 4 day 1, C1D1 cycle 1 day 1

corresponding GMR was 0.992 for the 4-h postdose sample, which was also not statistically different from 1 ($p > 0.05$) (Fig. 1). The mean \pm SD predose concentration on C1D1 (0.626 ± 0.540 ng/mL) and C4D1 (0.681 ± 0.745 ng/mL) was generally similar to corresponding values from the monotherapy studies [6]. These observations confirmed attainment of venetoclax steady state by the end of dose ramp-up, and indicated no time-dependent change in venetoclax CL/F over the first three cycles of venetoclax–rituximab, and no effect of rituximab on the PKs of venetoclax (Table 1, Fig. 1).

3.2 Dataset for Population PK Analysis

Among 194 patients randomized to venetoclax–rituximab in MURANO, 184 (94.8%) had one or more venetoclax PK observation records ($n = 643$ PK records). Exclusion of 11 (1.7%) observations collected > 10 days after the last dose, six (0.9%) postdose observations below LLOQ, and 26 (4.0%) with unreliable dosing information (missed doses during the week before sampling) left 600 quantifiable observation records, from 182 patients, for use in the population PK analysis. Electronic supplementary Fig. S1 shows the observed venetoclax plasma concentrations over time after the most recent dose. Patient covariates for the MURANO study and legacy model populations are summarized in Table 2 and electronic supplementary Table S1. Mean (range) bodyweight and age were 78.4 kg (41–115) and 63.9 years (28–83), respectively. Bodyweight and age correlated with creatinine CL (CRCL). Overall, 126 men (69.2%) and 56 women (30.8%) were included in the analysis. Male sex correlated with higher bodyweight and higher median age. Other continuous covariates were similarly distributed for male and female patients (electronic supplementary Figs. S2, S3). Most patients were White (96.7%), and six (3.3%) were Asian. Fifteen (8.2%) patients were from the US/Canada (region 1); 43 (23.6%) were from Australia/New Zealand (region 2); 60 (33.0%) were from Western Europe (region 3); 60 (33.0%) were from Eastern/

Table 1 Summary of venetoclax plasma concentrations ($\mu\text{g/mL}$) by visit (actual venetoclax dose = 400 mg)

Visit	No. of samples in the analysis ^a	No. of excluded samples	Mean (SD)	Range	%CV	Geometric mean (%CV)
Cycle 1 day 1						
Pre-venetoclax dose	151	6	0.626 (0.540)	0.0381–3.12	86.3	0.459 (96.8)
4 h post-venetoclax dose	159	10	1.34 (0.881)	0.0868–5.87	65.7	1.12 (66.6)
Cycle 4 day 1						
Pre-venetoclax dose	112	16	0.681 (0.745)	0.0500–4.83	109.5	0.472 (101.1)
4 h post-venetoclax dose	121	21	1.34 (0.905)	0.138–4.38	67.3	1.10 (73.5)

CV coefficient of variation, LTR less than reportable, SD standard deviation

^aSamples included LTRs

Central Europe (region 4); and four (2.2%) were from Asia (region 5). There were 42 (23.1%) patients with and 140 (76.9%) patients without del(17p). Ninety-six (52.7%) and 86 (47.3%) patients had high and low CLL risk, respectively.

3.3 Population PK Analysis

The prediction-corrected VPC plot (electronic supplementary Fig. S4) showed that the legacy model generally fitted the new data, although observed concentrations slightly exceeded model predictions. The model parameters were therefore re-estimated using Bayesian methodology, resulting in a 27-point decrease in objective function and an elimination of the slight underprediction of observed concentrations. Using this model as the reference, new covariates were tested using forward addition/backward elimination.

Use of a forward addition procedure resulted in a full model that included the effect of regions 1 and 3 on F_1 , and the effect of regions 4 and 5 on CL/F . The effect of regions 1 and 3 on F_1 was eliminated at the backward elimination step. Thus, the final model was identical to the legacy model, but with the additional effect of regions 4 and 5 on CL/F . Parameter estimates for the legacy and current final models, as well as the differences between them, are summarized in Table 3.

Figure 2 depicts the magnitude of the effects of the covariates incorporated into the final Bayesian model on AUC_{ss} (i.e. through CL/F or F_1):

- A minimal increase (mean 7%; 95% CI 2–12%) in the CL/F of venetoclax was observed after rituximab coadministration. CL/F was 30% lower (95% CI 21–39%) in patients from regions 4 ($n = 60$) or 5 ($n = 4$) compared with other regions. Strong CYP3A inhibitors decreased CL/F by 82% (95% CI 80–84%); moderate CYP3A inhibitors decreased CL/F by 14% (95% CI 7–21%); and OATP1B3 hepatic uptake transporter inhibitors decreased CL/F by 15% (95% CI 10–19%).
- V_2/F was 30% lower (95% CI 22–38%) in females ($n = 56$) than in males ($n = 126$).
- F_1 was fixed as 1 for the 400 mg dose with a low-fat meal. Administration in the fasting state decreased F_1 by 67% (95% CI 66–67%) relative to the low-fat postprandial state. Moderate- and high-fat meals increased F_1 by 36% (95% CI 14–56%) and 43% (95% CI 40–47%), respectively.
- $t_{1/2}$ was estimated at 1.07 days (25.7 h).

In the final model evaluation, goodness-of-fit of the data was confirmed (Fig. 3a), with no apparent model deficiencies. The conditional weighted residuals (CWRES) did not show any major trends when plotted against population-predicted values, with most values between ± 2 standard normal

deviations (Fig. 3a, panel 3), indicating that the model was appropriately unbiased and adequately described variability. Examination of the final model CWRES versus time (Fig. 3a, panel 6) indicated no apparent trend over time, confirming the lack of time-dependent PKs of venetoclax. The dependencies of the random effects on covariates did not show any further trends unaccounted for by the model (electronic supplementary Figs. S5–S10). This indicated that the trend observed in the plot of observed values versus individual predictions (DV vs. IPRED) can be explained by variability rather than systematic underprediction.

The VPC and NPDE plots (Fig. 3b, c) further supported good description of the observed MURANO study data by the Bayesian population PK model. The VPC plots of the simulated percentiles overlaid with the observed data, showing good agreement between the simulated and observed data, indicating that the model was able to describe the central tendency and variability of the data (Fig. 3b). The NPDE plots illustrated good predictive abilities of the model, with no dependencies of NPDE on time, time after dose, population predictions, or geographic region (Fig. 3c).

3.4 Individual PK Parameters

A summary of conditional predictions for PK parameters and steady-state exposure, overall and by geographic region, is shown in electronic supplementary Tables S2 and S3. Dependencies of individual estimates of CL/F on categorical and continuous covariates are illustrated in electronic supplementary Figs. S11 and S12. Consistent with the original population PK model, no relationship was observed between venetoclax CL/F and bodyweight, age, sex, mild or moderate hepatic and renal impairment, and coadministration of weak CYP3A inhibitors. However, a relationship was observed between CL/F and coadministration of strong CYP3A inhibitors, moderate CYP3A inhibitors, and OATP1B3 hepatic uptake transporter inhibitors. Venetoclax CL/F appeared lower in patients from regions 4 and 5. The new tested covariates of CLL risk status and del(17p) had no apparent effect on venetoclax exposure (Fig. 4).

4 Discussion

The result from the Bayesian model was very similar to the previously described legacy population PK model [6, 14], except that geographic region was added as a covariate on CL/F . Only patients with CLL were included in the current model, whereas the legacy analysis [6, 14, 23, 24] included healthy subjects and patients with CLL, SLL, multiple myeloma, or non-Hodgkin lymphoma (NHL). Venetoclax observed plasma concentrations were also comparable with those previously described [6, 25–27]. The observed data

Table 2 Continuous and categorical covariates at baseline. Covariate descriptions are followed by the covariate identifiers used in the model (in parentheses)

Continuous covariates	Measure	Result
Patients (<i>N</i>)	Number	182
Age (AGE), years	Mean (SD)	63.9 (10.6)
	Median (range)	65 (28–83)
Bodyweight (WTKG), kg	Mean (SD)	78.4 (14.1)
	Median (range)	77 (41–115)
Aspartate aminotransferase (AST), U/L	Mean (SD)	25.5 (11.8)
	Median (range)	23 (5–95)
Alanine aminotransferase (ALT), U/L	Mean (SD)	20.7 (10.9)
	Median (range)	18 (5–77.4)
Bilirubin (BILI), mg/dL	Mean (SD)	0.693 (0.434)
	Median (range)	0.585 (0.175–2.398)
Creatinine clearance (CRCL), mL/min	Mean (SD)	86.5 (24.7)
	Median (range)	83.8 (38–182.9)
Serum albumin (ALB), g/dL	Mean (SD)	4.11 (0.489)
	Median (range)	4.14 (2.4–5.27)
Categorical covariates	Level	<i>N</i> (%)
Sex (SEX)	Males	126 (69.2)
	Females	56 (30.8)
Race (RACE)	White	176 (96.7)
	Asian	6 (3.3)
Renal impairment (RENA_FN)	Normal	71 (39)
	Mild	91 (50)
	Moderate	20 (11)
Hepatic impairment (HEP_FN)	Normal	137 (75.3)
	Mild	34 (18.7)
	Moderate	11 (6)
Rituximab administration (RTX)	Not administered	4 (2.2)
	Administered	178 (97.8)
17p deletion (DEL17P)	No	140 (76.9)
	Yes	42 (23.1)
CYP3A inhibitor flag (C3AHIB) ^a	Not administered	30 (16.5)
	Weak	128 (70.3)
	Moderate	19 (10.4)
	Strong	5 (2.7)
OATP1B3 inhibitor flag (OATP3HIB) ^a	Not administered	177 (97.3)
	Administered	5 (2.7)
PGP inhibitor flag (PGPHIB)	Not administered	173 (95.1)
	Administered	9 (4.9)
CLL risk category (RISK) ^b	High	96 (52.7)
	Low	86 (47.3)
Region	USA/Canada	15 (8.2)
	Australia/New Zealand	43 (23.6)
	Western Europe	60 (33)
	Central/Eastern Europe	60 (33)
	Asia	4 (2.2)

Table 2 (continued)

Missing continuous covariates were imputed as the median value of the covariate, while missing categorical covariates were imputed as the most frequent value in the population. There were no covariates with a missing data fraction exceeding 15% of the study data

CLL chronic lymphocytic leukemia, CYP3A cytochrome P450 3A, OATP1B3 organic anion transporting polypeptide 1B3, PGP P-glycoprotein, SD standard deviation

^aStratification of inhibition as moderate or strong was based on US FDA guidance, as per the earlier analysis upon which the legacy model was based [6]. Details of the inhibitors used within the dataset are given in electronic supplementary Table S4

^bHigh CLL risk was defined as harboring del(17p), or no response to first-line chemotherapy, or relapse within 12 months of chemotherapy or 24 months of chemoimmunotherapy. Low CLL risk was defined as relapse more than 12 months after chemotherapy or 24 months after chemoimmunotherapy

analysis confirmed that steady-state plasma venetoclax concentrations were achieved after dose ramp-up, which is consistent with the reported linear PKs of venetoclax at 400 mg with a half-life of 26 h [6]; steady state was maintained at C4D1 (last PK assessment). No time-dependent change in venetoclax CL/F was apparent over the first three cycles of venetoclax–rituximab treatment. The similarity in predose venetoclax concentrations at C1D1 and C4D1 suggests that rituximab has no clinically relevant effect on venetoclax PKs, in line with the theoretical expectation.

Venetoclax apparent V_2/F was estimated to be 30% lower in females than in males, but this had no clinically relevant effect on steady-state exposure ($C_{\max,ss}$, $C_{\text{trough},ss}$, and AUC_{ss}) [electronic supplementary Fig. S13]. No clinically meaningful differences in the venetoclax–rituximab treatment arm were observed for efficacy and all-grade, grade 3 or higher, or serious adverse event rates, when stratified by sex [15]. Dosage adjustments based on sex are therefore not needed.

Consistent with the legacy model [6, 14], no apparent relationship was observed between venetoclax CL/F and bodyweight, age, sex, mild or moderate hepatic and renal impairment, and coadministration of weak CYP3A inhibitors. Mutation status [del(17p)] and CLL risk status had no influence on venetoclax CL/F. There is therefore no need for venetoclax dosage adjustments in these subgroups.

Although both healthy and malignant B cells can be bound and cleared by rituximab, this was not expected to impact on venetoclax PKs but was shown to potentiate venetoclax activity [28]. The CLL, SLL, and NHL disease indications, which have varying levels of circulating diseased B cells, had no effect on venetoclax PKs [6], suggesting a minimal effect of peripheral blood B-cell levels on venetoclax PKs (although this was not specifically tested as a covariate in the current and legacy population PK analyses). Disease-independent venetoclax PKs are also consistent with venetoclax steady-state exposures that

Table 3 Parameter estimates for the previous legacy [14] and the final current model, and the differences between them

Parameter	Final model (model 027)					Legacy model					Parameter estimate difference between the models (%)
	Final model estimate	RSE (%)	95% CI	Variability	Shrinkage	Legacy model estimate	RSE (%)	Variability	Shrinkage		
	CL/F (L/day)	469	2.79	443–495	–	–	447	3.51	–	–	
$\theta_{CL/F}$ -strong CYP3A inhibitor	0.182	5.66	0.162–0.203	–	–	0.184	6.03	–	–	–1.0	
$\theta_{CL/F}$ -moderate CYP3A inhibitor	0.859	4.07	0.791–0.928	–	–	0.842	4.24	–	–	2.1	
$\theta_{CL/F}$ -OATP1B3 inhibitor	0.853	FIXED	–	–	–	0.853	2.54	–	–	–	
$\theta_{CL/F}$ -rituximab	1.07	2.18	1.02–1.12	–	–	1.22	2.93	–	–	–12.3	
$\theta_{CL/F}$ -REGION=Central and Eastern Europe or Asia	0.696	6.62	0.606–0.786	–	–	–	–	–	–	–	
V_2/F (L)	118	13.6	86.4–149	–	–	118	13.7	–	–	0	
$\theta_{V_2/F}$ -CLL&LL&NHL	1.7	12.3	1.29–2.11	–	–	1.71	12.5	–	–	–0.6	
$\theta_{V_2/F}$ -SEX=female	0.7	6.02	0.618–0.783	–	–	0.680	6.68	–	–	2.9	
Q/F (L/day)	100	5.43	89.4–111	–	–	97.2	5.54	–	–	2.9	
V_3/F (L)	123	4.01	113–133	–	–	119	4.16	–	–	3.4	
k_a (1/day)	3.69	4.02	3.4–3.98	–	–	3.72	4.09	–	–	–0.8	
$\theta_{FI,FOOD}$ =fasting	0.335	0.965	0.329–0.341	–	–	0.335	0.967	–	–	0.0	
$\theta_{FI,FOOD}$ =moderate-fat	1.36	8.13	1.14–1.58	–	–	1.31	8.24	–	–	3.8	
$\theta_{FI,FOOD}$ =high-fat	1.43	1.29	1.4–1.47	–	–	1.43	1.30	–	–	0.0	
$\theta_{FI,FOOD}$ =fed ^a	1.27	3.98	1.17–1.37	–	–	1.23	4.29	–	–	3.3	
$F_{1,DOSE}$ nonlinearity (400 mg as reference)	–0.183	2.32	–0.191 to –0.175	–	–	–0.180	2.38	–	–	0.02	
$\omega^2_{CL/F}$	0.139	8.64	0.115–0.163	CV = 37.3%	30.3%	0.153	9.346	CV = 39.1%	19.0%	–9.2	
$\omega^2_{V_2/F}$	0.179	6.15	0.158–0.201	CV = 42.3%	54.3%	0.205	6.341	CV = 45.3%	27.7%	–12.7	
$\omega^2_{F_1}$	0.101	12.6	0.0759–0.126	CV = 31.7%	40.6%	0.0972	13.374	CV = 31.2%	28.3%	3.9	
σ^2_{prop}	0.219	1.61	0.212–0.226	CV = 46.8%	25.6%	0.223	1.67	–	–	–1.8	
σ^2_{add}	3.03×10^{-7}	39.7	0.674×10^{-7} to 5.38×10^{-7}	SD = 5.5×10^{-4}	25.6%	3.07×10^{-7}	39.7	–	–	–1.3	
Derived parameter											
$t_{1/2}$ (day)	1.07	–	–	–	–	–	–	–	–	–	

CI confidence interval, CL/F apparent clearance, CLL chronic lymphocytic leukemia, CV coefficient of variation, $CYP3A$ cytochrome P450 3A, F_1 relative bioavailability ($F_1 = 1$ corresponds to 400 mg with low-fat food), k_a first-order absorption rate constant, NHL non-Hodgkin lymphoma, $OATP1B3$ organic anion transporting polypeptide 1B3, Q/F apparent intercompartmental clearance, RSE residual standard error, SD standard deviation, SLL small lymphocytic lymphoma, $t_{1/2}$ terminal elimination half-life, V_2/F apparent central volume of distribution, V_3/F apparent peripheral volume of distribution, θ NONMEM fixed effect parameter, ω^2 interindividual variances, σ^2 residual variances

^aWithout specification of fat content

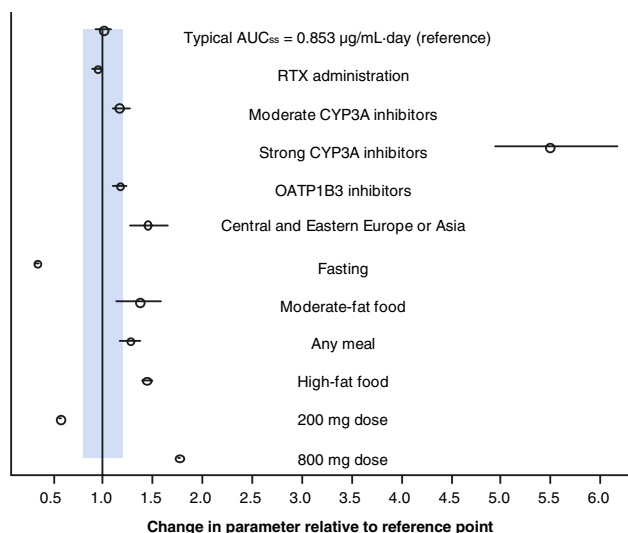


Fig. 2 Covariate effects on AUC_{ss} for the final model. Reference: 400 mg dose with low-fat food; USA/Canada, Australia/New Zealand, Western Europe. Ratio of the typical parameter and its 95% CI for subpopulations to the typical parameter of a reference patient is illustrated. For categorical covariates and continuous covariates with a specific value, point estimates = open circles, and 95% CIs = horizontal bars. The hatched area represents the typical value $\pm 20\%$. OATP1B3 was a fixed parameter. CYP3A cytochrome P450 3A, OATP1B3 organic anion transporting polypeptide 1B3 transporter, RTX rituximab, CI confidence interval, AUC_{ss} area under the curve of plasma venetoclax concentration versus time at steady state

increase approximately in proportion to dose over the range of 300–900 mg [29].

Consistent with a low observed potential for rituximab to impact venetoclax PKs, CL/F was increased by 7% with rituximab coadministration, which was lower than that determined in the previous analysis of Jones et al. (21%; 95% CI 14–28%) [6]. The previous study used 7483 plasma venetoclax samples from 505 patients, of whom only 50 had coadministration of rituximab. In contrast, all patients but one in the present analysis received rituximab, thus yielding considerably more robust combination therapy data. Therefore, the 7% rituximab effect determined in the present analysis provides the most reliable estimate of the potential impact of rituximab on venetoclax PKs, which is not expected to be clinically meaningful. This is also consistent with observed ratios of approximately 1.0 between C1 and C4 for predose concentrations of venetoclax.

Patients from Central and Eastern Europe or Asia were estimated to have 30% lower CL/F than patients from Western Europe, US/Canada, or Australia/New Zealand, which translates to approximately 43% greater venetoclax exposure. However, we note that there were only four patients from Asia in the MURANO dataset. Regional differences in implementation of the MURANO protocol-specified low-fat meal might have contributed to this geographic effect,

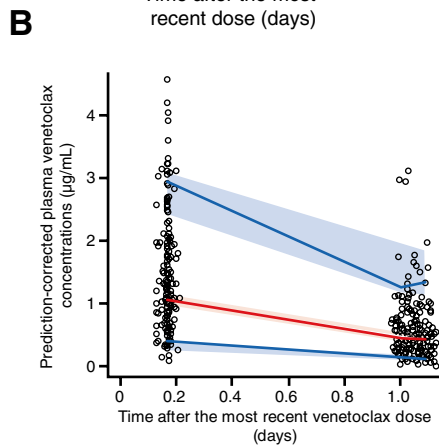
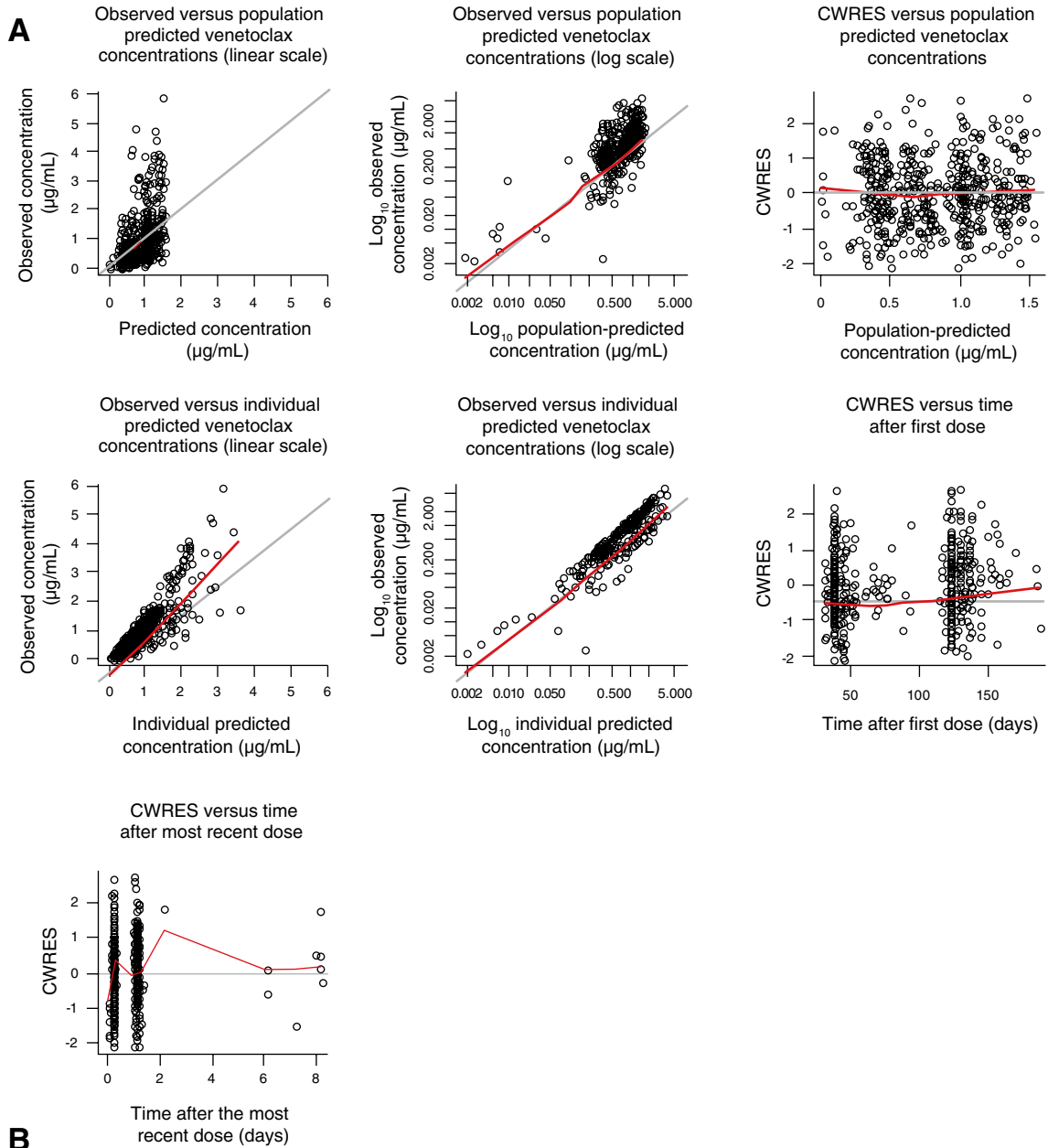
Fig. 3 Final model evaluation. **a** Goodness-of-fit plot for the final model; **b** prediction-corrected VPC plots for the final model; **c** NPDE plots for the final model. **a** The grey solid lines (showing plots of $y=x$ or $y=0$, as appropriate) are included for reference. The bold red lines are the LOWESS (local regression smoother) trend lines. **b** Points represent the prediction-corrected observed C_{ven} versus time after the most recent venetoclax dose. Red line represents the median, and blue lines represent the 5th and 95th percentiles of prediction-corrected observed C_{ven} . Shading = 90% confidence intervals (simulated from 500 trials with dosing, sampling, and covariate values of the analysis dataset). **c** NPDE versus time from the first dose, time after the most recent dose, population predictions, and geographic region. Circles correspond to the NPDE of observations in the distribution of 500 simulated values. Lines at $y=0$ correspond to the median values, and dashed lines show the 10th and 90th percentiles. Percentages of points below the 10th percentile and above the 50th and 90th percentiles are reported. Red lines show the LOWESS trend lines. Geographic region: 1 = USA/Canada; 2 = Australia/New Zealand; 3 = Western Europe; 4 = Central /Eastern Europe; and 5 = Asia. CWRES conditional weighted residuals, VPC visual predictive check, NPDE normalized prediction distribution error, C_{ven} venetoclax concentrations

although no definitive reason has been established. Moreover, subgroup analysis of efficacy and safety, by region, indicated that treatment benefit of equivalent magnitude in favor of the venetoclax–rituximab arm was observed across all evaluated regions [15]. Given that exposure–response analyses of venetoclax safety, tolerability, and efficacy parameters have shown no significant relationships with venetoclax exposure [30], this difference in venetoclax CL/F was not considered clinically relevant. Therefore, no dosage adjustment for venetoclax based on geographic region is felt to be necessary.

Other observations included an approximate 82% decrease in CL/F with administration of strong CYP3A inhibitors, and an approximate 14% decrease with moderate inhibitors. This finding was expected from the previous pooled analysis [6] and the known PK characteristics of venetoclax [3]. It provides support for existing dosage recommendations for venetoclax when administered with CYP3A inhibitors [3]. Of note, the dataset for the present analysis included data from only five patients with strong CYP3A inhibitor usage, and 19 with moderate CYP3A inhibitor usage. Therefore, the estimated covariate effects for CYP3A inhibitors was driven almost entirely by the legacy model, with the new dataset providing very little additional information.

The present model's estimate of effect of meal type on $F1$ and effect of patient population on CL/F were also strongly driven by the legacy model, given that all patients contributing new data (i.e. from MURANO) were receiving low-fat meals per the protocol and had relapsed/refractory CLL.

Shrinkage indicates whether the model is overparameterized for the amount of information contained in the data. When sparse PK sampling is performed, some PK



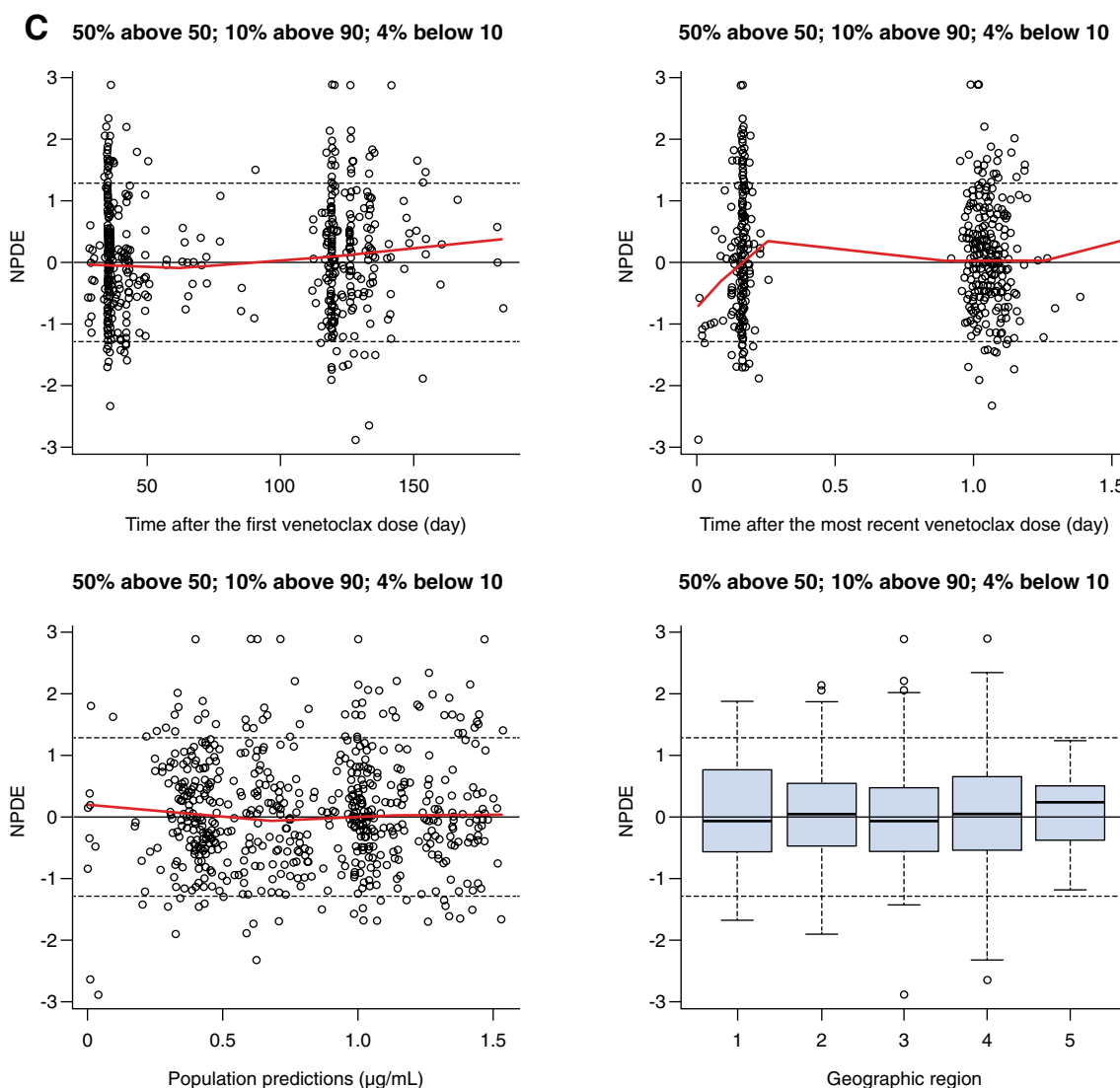


Fig. 3 (continued)

parameters may be better informed by the observed data than others, with high shrinkage to the population prediction for the less-informed parameters. In this study, shrinkage ranged from approximately 25% to approximately 50% for the current model (Table 3). This was considered acceptable given that only four PK samples per patient were collected in the MURANO study. Importantly, the shrinkage for the CL/F to $F1$ ratio, the key parameter for steady-state exposure calculations used in exposure–response analysis, was only 13.4%. This indicates that the current model provides a good estimate of individual steady-state PK exposures, further increasing confidence in the value of subsequent exposure–response analyses.

The present analysis was distinguished from previous work by the application of Bayesian techniques. In a Bayesian analysis, the likelihood that a set of parameters

is consistent with the observed data is calculated by multiplying the corresponding likelihood function by the prior distribution, and the result normalized to create a posterior distribution, from which final parameter estimates are obtained [31–33].

When an existing population PK model is available and structural changes to the model are not required, the Bayesian approach provides an efficient and scientifically strong alternative to a pooled analysis when extending a population PK analysis to a new dataset. As the population PK analysis dataset only needs to contain the new data, this approach simplifies the otherwise time-consuming dataset preparation step that can comprise the majority of effort for a typical pooled analysis. This could be important, for example, in an accelerated filing scenario, which is the case for MURANO.

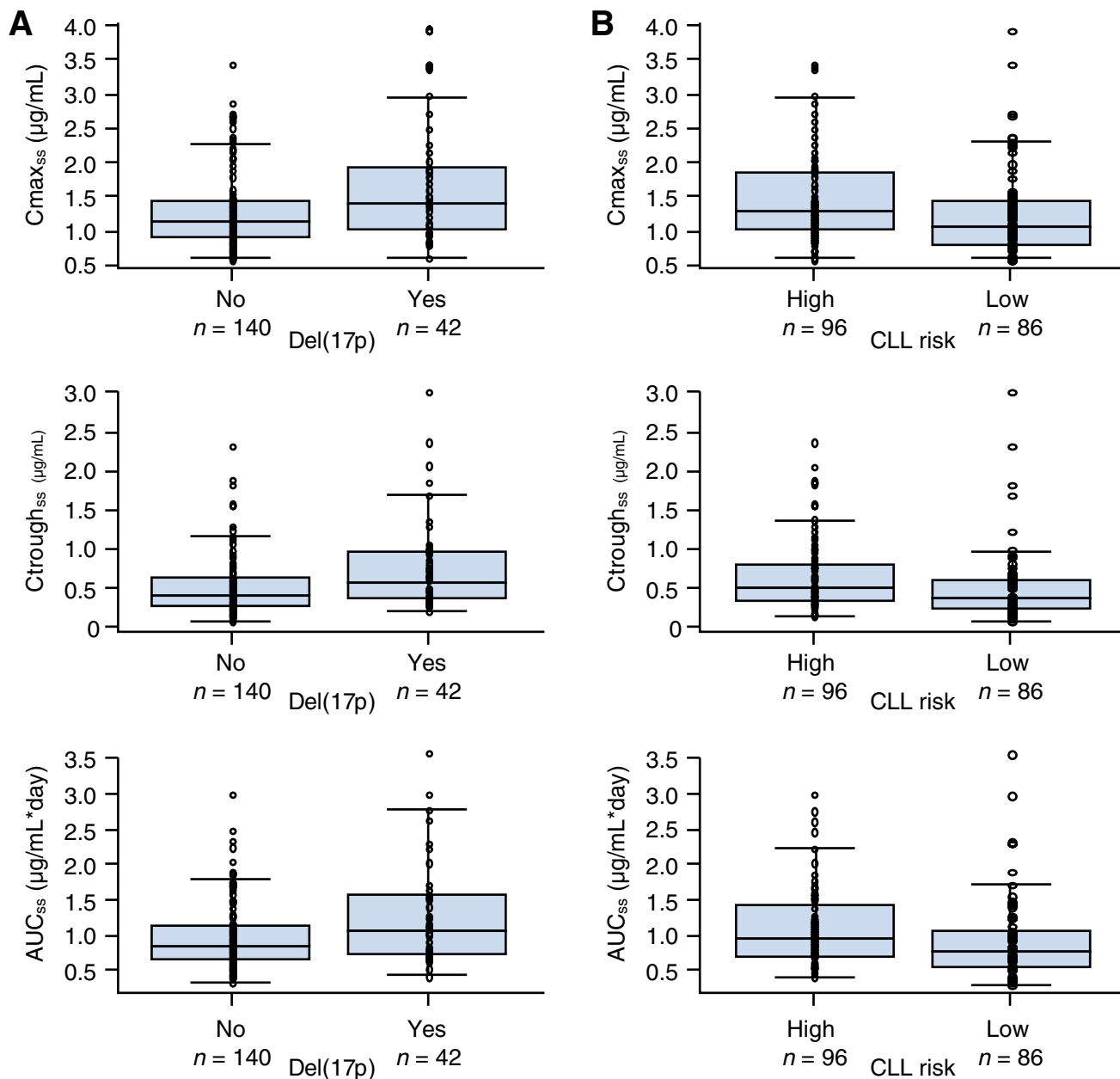


Fig. 4 Venetoclax $C_{max,ss}$, $C_{trough,ss}$, and AUC_{ss} by **a** 17p deletion mutation status [del(17p); 0=no 17p deletion, 1=17p deletion] and **b** CLL risk status (1=high risk, 2=low risk). Heavy black horizontal lines represent the median values; *boxes* represent the IQRs; and whiskers represent $1.5 \times IQR$. $C_{max,ss}$ peak plasma concentra-

tion at steady state, $C_{trough,ss}$ trough plasma concentration at steady state, AUC_{ss} area under the plasma concentration versus time curve at steady state, *CLL* chronic lymphocytic leukemia, *IQR* interquartile range

In the Bayesian analysis, new covariates (e.g. geographic region) that were relevant to both the legacy and MURANO datasets were tested. Whereas in a pooled analysis these types of covariates could have been informed by both legacy and new data, these covariates are only informed by the new data when a Bayesian analysis is employed. The strength of the Bayesian evaluation depends on how well the new

covariate is represented in the new data, and on the number/quality of the associated PK samples. Additionally, unlike models without priors (where one level of a categorical covariate serves as a reference), the effect of each level of a categorical covariate was tested individually and simultaneously within the same run, and then, if positive, investigated further. One potential drawback is that interpretation of the

covariate effect may be more complicated than in a typical pooled analysis (where one level serves as reference), depending on which covariate levels test positive.

In our analysis, the Bayesian approach provided a novel and flexible way to describe the MURANO data while minimizing the work related to dataset preparation for an accelerated filing. This was critical in order to bring this valuable treatment option to patients with a high unmet need. Model evaluation and diagnostics, including the prediction-corrected VPC plot (Fig. 3b) and the observed consistency in PK parameters between the current and legacy models [6, 14], support the use of the Bayesian model for describing the PKs of venetoclax in combination with rituximab.

5 Conclusions

A Bayesian population PK modeling approach provided a fast and efficient method for characterizing venetoclax concentration-time profiles in combination with rituximab, and for evaluating covariates. The findings were consistent with both the legacy population PK model and the analysis of observed venetoclax concentrations from the MURANO study. The model showed a minimal impact of rituximab on venetoclax CL/F , which was not considered clinically relevant. Therefore, no dosage adjustment is recommended for venetoclax in patients receiving concomitant rituximab. The model was deemed appropriate for generating post hoc exposure parameters for further use in simulations or for evaluation of exposure–response relationships.

Data Availability Qualified researchers may request access to individual patient-level data through the clinical study data request platform (<http://www.clinicalstudydatarequest.com>). Further details on Roche's criteria for eligible studies are available at <https://clinicalstudydatarequest.com/Study-Sponsors/Study-Sponsors-Roche.aspx>. For further details on Roche's Global Policy on the Sharing of Clinical Information and how to request access to related clinical study documents, see https://www.roche.com/research_and_development/who_we_are_how_we_work/clinical_trials/our_commitment_to_data_sharing.htm.

Acknowledgements Special thanks to the patients and their families, investigators, study coordinators, and support staff, and the MURANO study team members. The authors also thank Dr. Mehrdad Mobasher for his valuable contributions to the manuscript. Venetoclax is being developed in collaboration between Genentech, Inc. and AbbVie. Genentech and AbbVie provided financial support for the study and participated in the design, study conduct, analysis, and interpretation of data, as well as the writing, review, and approval of the manuscript. Third-party medical writing assistance was provided by Christopher Dunn and Andrew Sutton of Gardiner-Caldwell Communications, and was funded by F. Hoffmann-La Roche Ltd.

Compliance with Ethical Standards

Funding Genentech and AbbVie provided financial support for this study.

Conflict of interest Rong Deng, Tong Lu, Dan Lu, Chunze Li, Sandhya Girish, Jue Wang, and Dale Miles are employees of Genentech and have equity in Genentech/F. Hoffmann-La Roche Ltd. Leonid Gibiansky received consultancy fees from Genentech. Priya Agarwal and Xiaobin Li are employees of Genentech. Hao Ding and Smita Kshirsagar are paid contractors of Genentech. Michelle Boyer is an employee of F. Hoffmann-La Roche Ltd and has equity in the company. Kathryn Humphrey is an employee of F. Hoffmann-La Roche Ltd. Kevin J. Freise and Ahmed Hamed Salem are employees of AbbVie and have equity in the company. John F. Seymour received grants from AbbVie, Celgene, Janssen, and F. Hoffmann-La Roche Ltd; consultancy fees from AbbVie, Acerta, Celgene, Janssen, F. Hoffmann-La Roche Ltd, and Takeda; travel support from AbbVie; advisory board fees from Celgene; lecture/speakers' bureau fees from AbbVie and F. Hoffmann-La Roche Ltd; and expert testimony fees from F. Hoffmann-La Roche Ltd. Arnon P. Kater received grants from F. Hoffmann-La Roche Ltd, Genentech, and AbbVie; consultancy fees from AbbVie; travel support from F. Hoffmann-La Roche Ltd; and lecture/speakers' bureau fees from AbbVie.

Ethical approval All procedures performed in the MURANO study were in accordance with the ethical standards of the institutional and/or national research committee and with the 1964 Helsinki declaration and its later amendments or comparable ethical standards.

Informed consent Informed consent was obtained from all individual participants included in the MURANO study.

References

1. Souers AJ, Levenson JD, Boghaert ER, Ackler SL, Catron ND, Chen J, et al. ABT-199, a potent and selective BCL-2 inhibitor, achieves antitumor activity while sparing platelets. *Nat Med*. 2013;19:202–8.
2. Deeks ED. Venetoclax: first global approval. *Drugs*. 2016;76:979–87.
3. Highlights of prescribing information. VENCLEXTA™ (venetoclax) tablets, for oral use. Initial US Approval: 2016. Revised: June 2018. North Chicago, IL: Abbvie Inc.
4. Agarwal SK, Hu B, Chien D, Wong SL, Salem AH. Evaluation of rifampin's transporter inhibitory and CYP3A inductive effects on the pharmacokinetics of venetoclax, a BCL-2 inhibitor: results of a single- and multiple-dose study. *J Clin Pharmacol*. 2016;56:1335–43.
5. Freise KJ, Jones AK, Eckert D, Mensing S, Wong SL, Humerickhouse RA, et al. Impact of venetoclax exposure on clinical efficacy and safety in patients with relapsed or refractory chronic lymphocytic leukemia. *Clin Pharmacokinet*. 2017;56:515–23.
6. Jones AK, Freise KJ, Agarwal SK, Humerickhouse RA, Wong SL, Salem AH. Clinical predictors of venetoclax pharmacokinetics in chronic lymphocytic leukemia and non-Hodgkin's lymphoma patients: a pooled population pharmacokinetic analysis. *AAPS J*. 2016;18:1192–202.
7. Salem AH, Hu B, Freise KJ, Agarwal SK, Sidhu DS, Wong SL. Evaluation of the pharmacokinetic interaction between venetoclax, a selective BCL-2 inhibitor, and warfarin in healthy volunteers. *Clin Drug Investig*. 2017;37:303–9.

8. Salem AH, Agarwal SK, Dunbar M, Enschede SL, Humerickhouse RA, Wong SL. Pharmacokinetics of venetoclax, a novel BCL-2 inhibitor, in patients with relapsed or refractory chronic lymphocytic leukemia or non-Hodgkin lymphoma. *J Clin Pharmacol*. 2017;57:484–92.
9. Agarwal SK, DiNardo CD, Potluri J, Dunbar M, Kantarjian HM, Humerickhouse RA, et al. Management of venetoclax-ponasaconazole interaction in acute myeloid leukemia patients: evaluation of dose adjustments. *Clin Ther*. 2017;39:359–67.
10. Freise KJ, Hu B, Salem AH. Impact of ritonavir dose and schedule on CYP3A inhibition and venetoclax clinical pharmacokinetics. *Eur J Clin Pharmacol*. 2018;74:413–21.
11. Agarwal SK, Salem AH, Danilov AV, Hu B, Puvvada S, Gutierrez M, et al. Effect of ketoconazole, a strong CYP3A inhibitor, on the pharmacokinetics of venetoclax, a BCL-2 inhibitor, in patients with non-Hodgkin lymphoma. *Br J Clin Pharmacol*. 2017;83:846–54.
12. Freise KJ, Shebley M, Salem AH. Quantitative prediction of the effect of CYP3A inhibitors and inducers on venetoclax pharmacokinetics using a physiologically based pharmacokinetic model. *J Clin Pharmacol*. 2017;57:796–804.
13. Liu H, Michmerhuizen MJ, Lao Y, Wan K, Salem AH, Sawicki J, et al. Metabolism and disposition of a novel B-cell lymphoma-2 inhibitor venetoclax in humans and characterization of its unusual metabolites. *Drug Metab Dispos*. 2017;45:294–305.
14. Center for Drug Evaluation and Research. Application number: 208573Orig1s000. Clinical pharmacology and biopharmaceutics review(s). NDA 208573 Venetoclax. Reference ID: 3901940. 2015. https://www.accessdata.fda.gov/drugsatfda_docs/nda/2016/208573Orig1s000ClinPharmR.pdf. Accessed 6 Nov 2018.
15. Seymour JF, Kipps TJ, Eichhorst B, Hillmen P, D’Rozario J, Assouline S, et al. Venetoclax-rituximab in relapsed or refractory chronic lymphocytic leukemia. *N Engl J Med*. 2018;378:1107–20.
16. International Conference on Harmonisation of Technical Requirements for Registration of Pharmaceuticals for Human Use (ICH) adopts consolidated guideline on good clinical practice in the conduct of clinical trials on medicinal products for human use. *Int Dig Health Legis*. 1997;48:231–4.
17. World Medical Association. World Medical Association Declaration of Helsinki: ethical principles for medical research involving human subjects. *JAMA*. 2013;310:2191–4.
18. Gisleskog PO, Karlsson MO, Beal SL. Use of prior information to stabilize a population data analysis. *J Pharmacokinet Pharmacodyn*. 2002;29:473–505.
19. Yano Y, Beal SL, Sheiner LB. Evaluating pharmacokinetic/pharmacodynamic models using the posterior predictive check. *J Pharmacokinet Pharmacodyn*. 2001;28:171–92.
20. Bergstrand M, Hooker AC, Wallin JE, Karlsson MO. Prediction-corrected visual predictive checks for diagnosing nonlinear mixed-effects models. *AAPS J*. 2011;13:143–51.
21. Brendel K, Comets E, Laffont C, Laveille C, Mentre F. Metrics for external model evaluation with an application to the population pharmacokinetics of gliclazide. *Pharm Res*. 2006;23:2036–49.
22. Beal S, Sheiner LB, Boeckmann A, Bauer RJ. NONMEM user’s guides (1989–2011). Ellicott City: Icon Development Solutions; 2011.
23. Freise KJ, Jones AK, Verdugo ME, Menon RM, Maciag PC, Salem AH. Moving beyond maximum tolerated dose for targeted oncology drugs: use of clinical utility index to optimize venetoclax dosage in multiple myeloma patients. *Clin Pharmacol Ther*. 2017;102:970–6.
24. Parikh A, Gopalakrishnan S, Freise KJ, Verdugo ME, Menon RM, Mensing S, et al. Exposure-response evaluations of venetoclax efficacy and safety in patients with non-Hodgkin lymphoma. *Leuk Lymphoma*. 2018;59:871–9.
25. Guinney J, Wang T, Laajala TD, Winner KK, Bare JC, Neto EC, et al. Prediction of overall survival for patients with metastatic castration-resistant prostate cancer: development of a prognostic model through a crowdsourced challenge with open clinical trial data. *Lancet Oncol*. 2017;18:132–42.
26. Wang B, Nichol JL, Sullivan JT. Pharmacodynamics and pharmacokinetics of AMG 531, a novel thrombopoietin receptor ligand. *Clin Pharmacol Ther*. 2004;76:628–38.
27. Kumagai Y, Fujita T, Ozaki M, Sahashi K, Ohkura M, Ohtsu T, et al. Pharmacodynamics and pharmacokinetics of AMG 531, a thrombopoiesis-stimulating peptibody, in healthy Japanese subjects: a randomized, placebo-controlled study. *J Clin Pharmacol*. 2007;47:1489–97.
28. Freise KJ, Jones AK, Menon RM, Verdugo ME, Humerickhouse RA, Awni WM, et al. Relationship between venetoclax exposure, rituximab coadministration, and progression-free survival in patients with relapsed or refractory chronic lymphocytic leukemia: demonstration of synergy. *Hematol Oncol*. 2017;35:679–84.
29. Salem AH, Dunbar M, Agarwal SK. Pharmacokinetics of venetoclax in patients with 17p deletion chronic lymphocytic leukemia. *Anticancer Drugs*. 2017;28:911–4.
30. Deng R, Gibiansky L, Lu T, Li X, Lu D, Li C, et al. Exposure-response analysis of venetoclax in combination with rituximab in patients with relapsed or refractory chronic lymphocytic leukemia: phase 3 MURANO study. American College of Clinical Pharmacology Conference; 23–25 Sep 2018: Bethesda, MD
31. Weisstein EW. Bayesian analysis. From MathWorld – A Wolfram Web Resource. <http://mathworld.wolfram.com/BayesianAnalysis.html>. Accessed 19 Dec 2018.
32. van de Schoot R, Kaplan D, Denissen J, Asendorpf JB, Neyer FJ, van Aken MAG. A gentle introduction to bayesian analysis: applications to developmental research. *Child Dev*. 2014;85:842–60.
33. Bolstad WM, Curran JM. Introduction to Bayesian statistics. 3rd ed. Hoboken: Wiley; 2017.

Affiliations

Rong Deng^{1,7} · Leonid Gibiansky² · Tong Lu¹ · Priya Agarwal¹ · Hao Ding¹ · Xiaobin Li¹ · Smita Kshirsagar¹ · Dan Lu¹ · Chunze Li¹ · Sandhya Girish¹ · Jue Wang¹ · Michelle Boyer³ · Kathryn Humphrey³ · Kevin J. Freise⁴ · Ahmed Hamed Salem⁴ · John F. Seymour⁵ · Arnon P. Kater⁶ · Dale Miles¹

¹ Genentech Inc., South San Francisco, CA, USA

² QuantPharm, LLC, North Potomac, MD, USA

³ Roche Products Limited, Welwyn Garden City, UK

⁴ AbbVie, North Chicago, IL, USA

⁵ Royal Melbourne Hospital, Peter MacCallum Cancer Centre, and University of Melbourne, Melbourne, VIC, Australia

⁶ Department of Hematology, Amsterdam UMC, University of Amsterdam on behalf of HOVON CLL WG, Amsterdam, The Netherlands

⁷ Clinical Pharmacology, Genentech Research and Early Development, 1 DNA Way, MS463a, South San Francisco, CA 94080, USA